International Journal of Nanoelectronics and Materials
Volume 15, No. 3, July 2022 [269-280]

Preparation and Investigation of Gold Nanoparticles by the Technique of Laser Ablation for Biological Application

Dhuha H. Al-Obaidi[1*], Olfat A. Mahmood[1], Ammar A. Habeeb[1], Mustafa Z. Abdullah[2]

[1]Faculty of Physics Science, University of Diyala, Diyala, Iraq
[2]Directorate of Materials Research, Ministry of Science and Technology, Baghdad, Iraq

Received 28 March 2012, Revised 17 April 2022, Accepted 6 May 2022

ABSTRACT

This paper utilises environmentally friendly and cost-effective methods for the synthesis of gold nanoparticles (AuNPs) using distilled water (DW) solution via liquid pulse laser ablation (PLAL) technique with wavelength (1064nm) and different laser energies. The properties of Au NPs were studied by using absorption spectrometry and its particle shape, surface morphology and size ratio were analysed by transmission electron microscopy (TEM) and X-ray diffraction. The prepared samples were examined by X-ray diffraction (XRD) and the analyses showed the formation of a crystal structure for gold (Fcc) and showed an improvement in the crystal level by increasing the energy of the laser beam, which leads to an increase in the grain size. The Uv_Vis results showed the formation of Au NPs through the appearance of the surface plasmon resonance (SPR) peak located at 523nm within the UV visible spectrum. Transmission electron microscopy (TEM) images showed Au NPs in a spherical or aspherical cluster shape with diameters ranging from 25 to 50 nm. Au NPs act as antibacterial against Staph aureus, and p.aeruginosa. This is due to the large surface-to-volume ratio which provides a more effective means of enhancing bacterial activity as measured by the area of inhibition.

Keywords: Pulsed Laser Ablation in Liquids, Distilled Water, Gold Nanoparticles

1. INTRODUCTION

Nanotechnology is defined as the evaluation and fabrication of nanomaterials and their applications for the links between their physical properties and material spacing [1]. On nanometer scale, materials or structures may show new physical phenomena or have new physical properties. Examples for these properties are semiconductors band gaps that can be modified by changing dimensions of materials, the melting point of crystals in nanometer scale is low and decreases constants of lattice, the number of surfaces ions or atoms becomes a significant fraction of the total number of ions or atoms, and the surface energy is especially important in the thermal stability.

Atoms or ions become an important part of the total number of ions and the surface energy in thermal stability, and all three dimensions of the particle are within the nanometer scale, where they are called nanoparticles (NPs) due to their sufficient and small number of molecules and atoms and differ from the properties in their counterpart mass and are in different shapes, including spherical and pentagonal, cubic or rod-shaped, shells and ellipsoidal [1]. The small nanoparticles called "Cluster" that have well-defined composition and surface structure as finite aggregates of atoms or molecules that are bound by metallic forces, hydrogen, covalent, ionic, or van der Waals bonds [2]. Noble metal

* Corresponding author: dhuha.alobaidi.22@gmail.com

NPs have gained much consideration because of their exclusive size dependent catalytic properties, optical properties and magnetic properties [3].

Due to these properties, noble metal NPs are used with many applications, like catalytic [3], biomedical applications [4], surface-enhanced Raman scattering (SERS) [5], drug delivery [6], antibacterial [7], biosensing [8]. There are many methods to synthesise and prepare the noble metal NPs chemically and physically like electrochemical method [9], wet chemistry [10], vapor deposition [11] and laser ablation [3]. Gold (Au) can be considered a universal, biologically inert metal but AuNPs have many biologically functions [12]. AuNPs can be obtained in different sizes and employed with the desired polymers where they are classified as biocompatible materials [13].

When AuNPs bind to the bacterial membrane, the contents will leak and penetrate the outer membrane and peptidoglycan layer, leading to the death of the bacteria [14]. When comparing with silver nanoparticles (AgNPs), we noticed that studies on antimicrobial AuNPs hydrogels are rare, as mentioned in a recent study [15]. Thus, in this study, we aim to prepare AuNPs particles in a simple way using PLAL technique of the target material by immersed in water, shedding different laser energies and verifying the effect of these energies on the size of nanoparticles and using them to examine the biological effect against two types of gram-positive and negative bacteria. Furthermore, we highlight the study of the structural, morphological and optical properties of AuNPs.

2. THE EXPERIMENTAL DETAILS

2.1 Method and materials used

2.1.1 Nd-YAG laser

A HUAFEI switched Nd-YAG laser system providing pulses with a wavelength of 1064 nm and a pulse width of 10 ns, a repetition rate of 1 Hz, the highest energy per pulse of 1000 mJ and an effective beam diameter of 2 mm, was used for laser ablation as shown in Figure 1 and Figure 2. The device is located in Department of Physics, College of Science, University of Diyala. The target used in this research is the high purity (99.9%) carat gold metal, with dimensions of 8.7 * 14.6 * 0.2 mm and weight 0.5 g as shown in Figure 3. The solutions used were pure medical distilled water (DW) solutions with a capacity of 5 ml prepared for each sample.

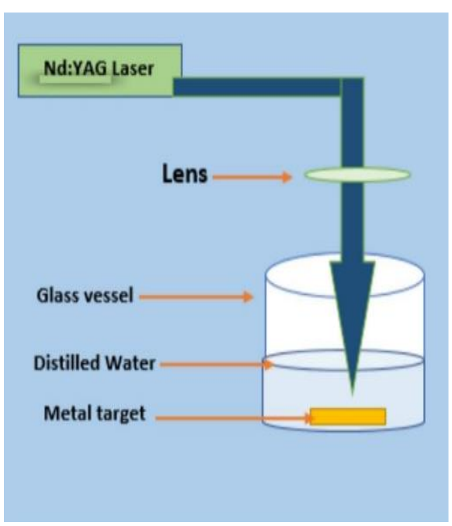

Figure 1. Scheme of the laser device **Figure 2.** Nd-YAG Laser

Figure 3. The gold target

2.1.2 Preparation of AuNPs

In this work, pulsed laser ablation technology (PLAL) was used to form particles of AuNPs by immersing the gold piece in a distilled water (DW) solution as a natural and environmentally friendly solvent compared to other organic solvents, and the target was with a high purity of 99.9% and suitable dimensions (8.7 * 14.6 * 0.2) mm with a weight of 0.5 gm, and the metallic gold was washed using pure water and chlorine benzene to remove the suspended pollutants on the surface, and it was immersed in the bowl with a quantity of water (5ml) and the target was irradiated using a ND:YAG laser with the following the parameters: Pulse width (2mm), wavelength (1064 nm), frequency (1 Hz), (550.600.650.700 mJ), and samples were prepared as in Figure 4.

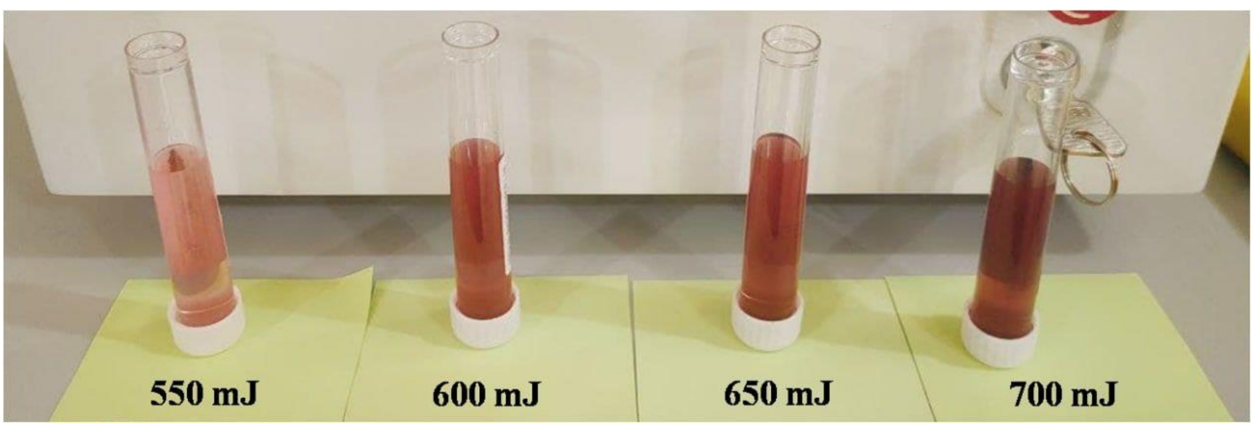

Figure 4. The prepared colloidal solutions are shown in different powers

3. CHARACTERIZATION TECHNIQUES

X-ray diffraction was characterized using Shimadzu-6000 at wavelength (°λ = 1.54060 A) and Cu Ka radiation (l ¼ 1.540 _A) system and the tube voltage was about 40 kV. Before performing the XRD test, the liquid is manually deposited by dripping on glass plates placed on a heater at 100°C. Transmission electron microscopy (TEM) was used to determine the surface morphology and shape of AuNPs and physical properties such as molar size, dispersion and diameter, which will be discussed. The intensity of absorption depends on the different ablation energy, where the higher the energy, the higher the absorbance, with the decrease in wavelength.

4. RESULTS AND DISCUSSION

4.1 X-ray diffraction test (XRD)

X-ray diffraction XRD was performed for samples prepared using an X-ray diffraction device type (Shimadzu- 6000) at wavelength (°λ = 1.54060 A) and effort difference (40 KV) .Figure 5 shows the X-ray diffraction patterns (XRD) for AuNPs prepared by laser extraction method at different energies (550, 600, 650, 700 mJ). The X-ray diffraction results showed that the characteristic peaks of AuNPs were obtained at these angles (2Θ = 38.39°, 44.75°, 65.96°, 77.84°) at the Crystal Planes (111) (200) (220) (311) respectively, ،with a space group (Fm-3m no.225) and dimensions (a=b=c= 4.0699 ˚A) and crystal angles (α=β=γ= 90 °) at the energies (600, 650, 700 mJ) which matches with the standard card (JCPDS 01-1172) .While at energy (550 mJ), AuNPs did not appear clearly during the X-ray diffraction test as shown in Figure 5. This is due to the fact that at high energies, the laser generates heat that is sufficient to form the cubic phase of Au NPs [16]. The reason for using high and low energies to ablate the material is to control the crystal size and particle size and to check the different crystallinity of the nanoparticles using different energies. No other peaks have been detected and this indicates that the obtained AuNPs are pure. From the results obtained, it was found that an increase in laser power led to crystallization increase in AuNPs as the phase became clearer and the characteristic peaks became sharper and more distinct, and the AuNPs continue its crystalline growth with the same cubic phase, as shown in Figure 5.

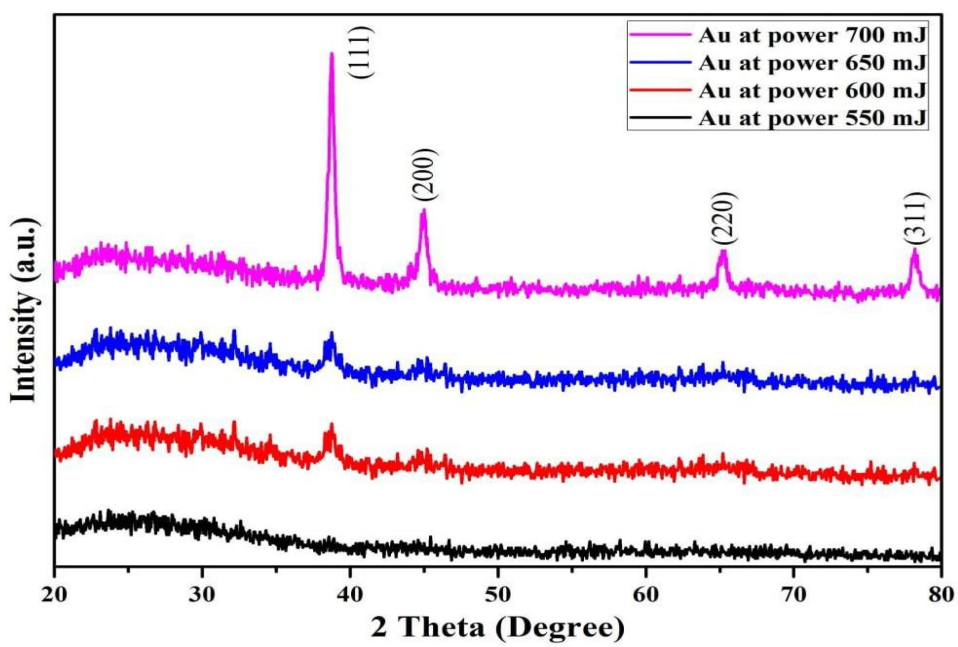

Figure 5. X-ray diffraction patterns (XRD) for Au NPs

Average crystalline size calculation was done using Scherrer equation (Debye-Scherrer) for AuNPs and the results are equal to 7.75 nm, 8.5 nm, 10.57 nm and 12.83 nm at the energies of 550, 600, 650, 700 mJ respectively. It is observed that the crystal size increases with increasing laser power, this is due to the increase in the crystalline growth due to increasing the temperature at higher energies and consequently increasing the crystalline size [17][18], and as shown in Table 1 which reviews the values of some crystalline parameters extracted from the X-ray diffraction test for AuNPs prepared at different energies.

Table 1 Some crystal parameters of Au NPs prepared at different energies

Au NPs at energy (700 mJ)						
2Θ (deg) Practical	2Θ (deg) Standard	FWHM (deg)	Crystalline size (nm)	d_{hkl} (°A) Practical	d_{hkl} (°A) Standard	(hkl)
38.39	38.26	0.51014	14.7	2.3428	2.35	(111)
44.75	44.6	0.63139	11.63	2.0235	2.03	(200)
65.96	64.67	0.46656	14.36	1.4344	1.44	(220)
77.84	77.54	0.58069	10.64	1.2261	1.23	(311)
Au NPs at energy (650 mJ)						
38.39	38.26	0.83774	8.95	2.3428	2.35	(111)
44.75	44.6	0.6988	10.51	2.0235	2.03	(200)
65.96	64.67	0.56298	11.9	1.4344	1.44	(220)
77.84	77.54	0.5642	10.95	1.2261	1.23	(311)
Au NPs at energy (600 mJ)						
38.39	38.26	0.77505	9.68	2.3428	2.35	(111)
44.75	44.6	0.80015	9.18	2.0235	2.03	(200)
65.96	64.67	0.82547	8.11	1.4344	1.44	(220)
77.84	77.54	0.87628	7.05	1.2261	1.23	(311)
Au NPs at energy (550 mJ)						
38.28	38.26	0.8391	8.94	2.3493	2.35	(111)
44.62	44.6	1.1187	6.56	2.0291	2.03	(200)

4.2 UV-Visible spectroscopy of AuNPs

UV-Visible spectroscopy is a method used for determining the amount of the light absorbed and scattered via sample. One of the important properties of nanoparticles is the optical properties in order to know specific information about concentration, state of agglomerations, size and shape. Figure 6 shows the UV-Visible spectra of AuNPs prepared by different laser energy, using the Nd:YAG laser 1064 nm with different energy of 550, 600, 650, and 700 mJ at constant pulse of 500 pulses. The spectra exhibit absorption band characteristic with peak located at around 521-523 nm for AuNPs. This is corresponding to SPR for gold [19]. The presence of single SPR peak is due to the NPs present in solution which are predominantly spherical in shape and non aggregated. The value of the plasmon peak increased with increasing laser energy. The intensity of SPR peak depends on the concentration of NPs in suspension, thus the higher concentration of NPs leads to higher value of the absorbance. We see the SPR peak is decreased, this means the NPs is reaching to critical size, when the laser energy of 550mJ due to the shielding effect when laser interact with solid surface, the temperature of solid increased leading to melting and evaporation happen plasma the part of laser absorbed in plasma so the laser energy reaching the target reduced that is called plasma shielding [20]. When laser energy exceeds 700mJ, the concentration begins to increase, so the absorption increased. Table 2 presents the experimental results of plasmon resonance, absorbance intensity and wavelength of 1064 nm.

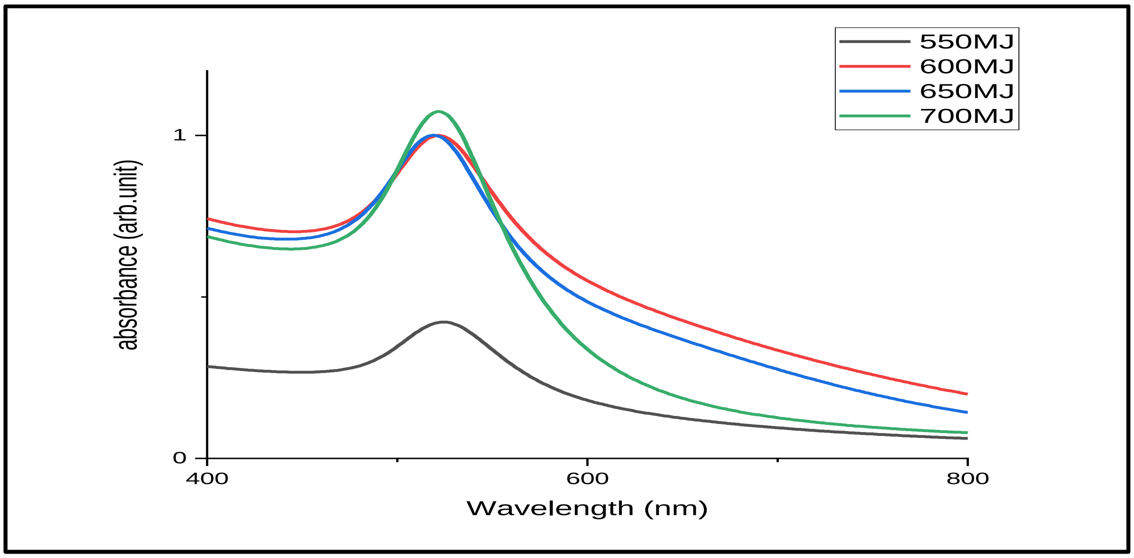

Figure 6. UV_ViS of Au NPs

Table 2 Surface plasmon resonance peak

Nanomaterials	number of laser pulses	Laser energy mJ	plasmon resonance SPR(nm)	Absorbance (nm)
AU 24	500	550	523	0.422
		600	521	1.000
		650	519	1.001
		700	521	1.074

4.3 Transmission Electron Microscopy (TEM)

Figure 7 shows TEM micrographs and their histograms and volume distribution for AuNPs prepared using PLAL technique. The nanoparticles appeared for different ablation energies of 550, 600, 650, 700 mJ which were consistent with UV-Vis and X-ray results in terms of particle size and crystallinity, where the high-density particles were clearly small clusters. In spherical shapes that were connected to each other and a network in some areas and a narrow distribution of size at low energies, the average particle diameters at energy 550 mJ equals to 18.1 nm as shown in Figure 7-D, and when the energy rises to 700 mJ, the size distribution of particle diameters increased to 45.5 nm as shown in Figure 7-A. This result means that the size of the as-prepared particles becomes larger with the increase of the ablation energy [21].

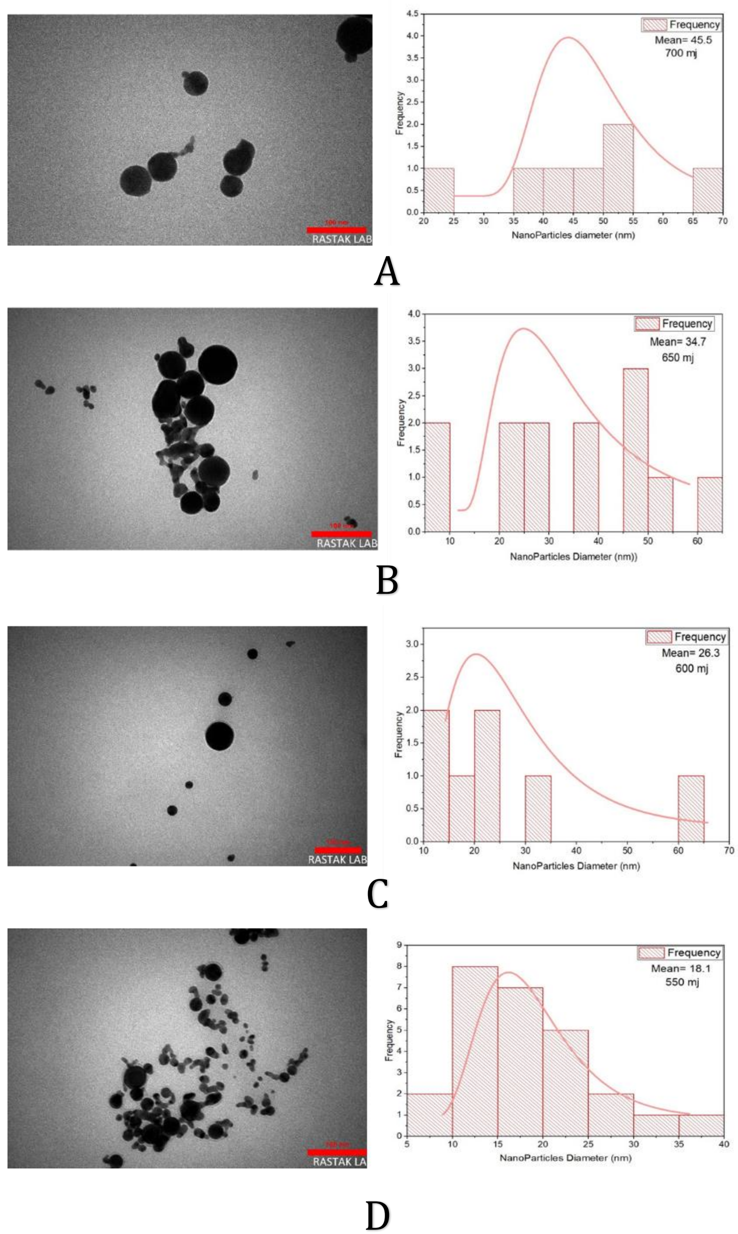

Figure 7. TEM photo for prepared AuNPs

5. ANTI-BACTERIAL AuNPs

In this work, the antibacterial activity of AuNPs was studied against two types of bacteria (Staph aureus and P.aeruginosa) negative and gram-positive, where the anti-particle property against bacteria was evaluated using standard agar diffusion technique using nanoparticle solution where the growth of bacteria strain was observed on the plate at 37° Celsius. The wells were drilled with diameters (6 mm) in the agar oasis. It was filled with a solution of nanoparticles. and spread it on nutrient agar plates and incubated at 37 °C for 24 hours. The number of CFU was counted as shown in Figure 8 and Table 3, and its histogram is as shown in Figure 9. This result is consistent with the result of previous researches [22][23][24][25]. It was more influential against gram-negative bacteria. The antibacterial mechanism of AuNPs against four pathogenic bacteria demonstrated that AuNPs can be the next therapy against this enteric bacterium, where the maximum zone of inhibition for AuNPs against Staph aureus and P.aeruginosa is 13 mm and 14 mm, respectively. It shows that the smaller the energy, the greater the amount of inhibition.

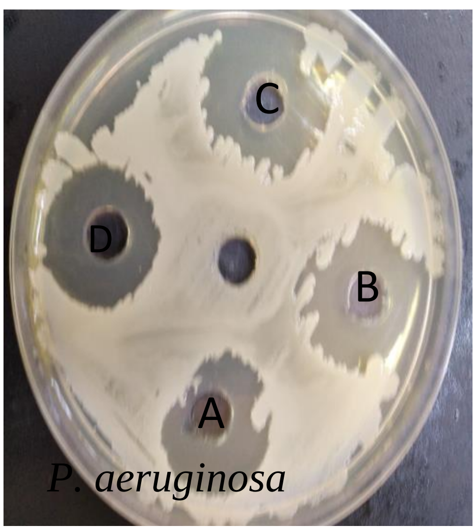

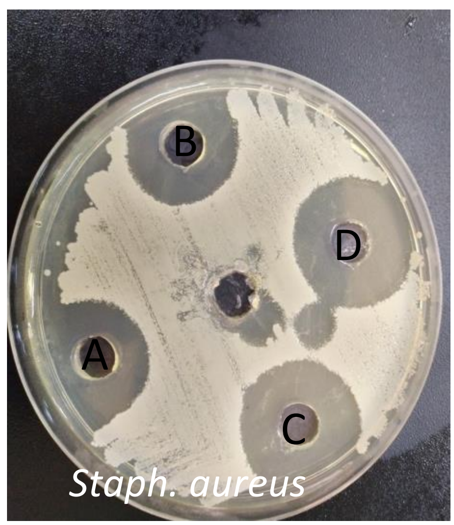

Figure 8. Antibacterial of AuNPs against two pathogen Staph aureus and P.aeruginosa by well diffusion method at different energy

Table 3 Antibacterial activity of AuNPs synthesised by laser ablation at different energy (550, 600,650 and 700) mJ against P. aeruginosa. and Staph. aureus.

Microorganisms	(Mean ± SD) Zone of inhibition (mm)				
	D (550 mJ)	**C (600 mJ)**	**B (650 mJ)**	**A (700 mJ)**	**Control**
Staph. Aureus	11.22±0.01	12.22±0.01	12.77±0.02	14.21±0.01*	-
P. aeruginosa	10.32±0.01	11.51±0.01	12.11±0.01	13.32±0.01	-

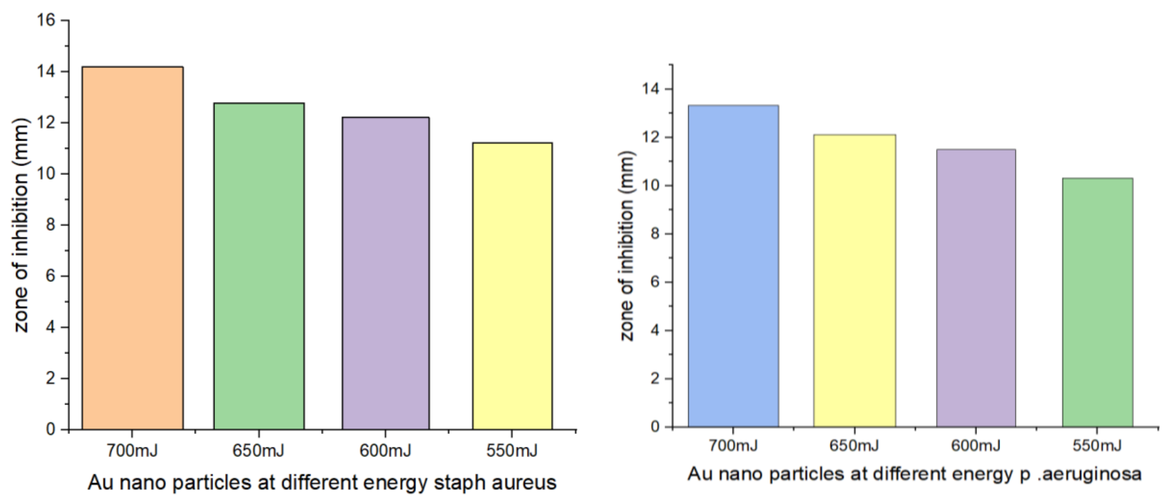

Figure 9. Laser energy

6. CONCLUSION

Liquid Pulsed Laser Ablation (PLAL) is an environmentally friendly and effective method for nanoparticle synthesis and is cost-effective. The measurements of the electron microscope (TEM) and XRD proved the formation of spherical AuNPs with a crystalline structure of Fcc and sizes ranging from 25 and 50 nm. Preparation of gold nanoparticles are by immersing in distilled water (DW) by PLAL using a pulsed laser device at a wavelength of 1064 nm and using nanoscale gold deposition techniques on glass to examine the results XRD. UV_VIS shows that with increasing energy, the surface plasmon resonance (SPR) peak of the AuNPs increases. The prepared gold nanoparticles AuNPs are affected by the energy of the laser beam, and as the energy increases, the size of the nanoparticles increases and begins to agglomerate. It is worth noting that gold nanoparticles have revolutionized the field of medicine for their wide applications in imaging, diagnosis delivery of targeted drugs and therapeutics, due to their small size, lack of cellular toxicity, high surface area and their physical, chemical and optical properties. The prepared AuNPs showed significant elevated level in antibacterial activities, where it shows that the greater the energy, the greater the amount of inhibition.

REFERENCES

[1] G. Cao, Nanostructures & nanomaterials: synthesis, properties & applications. Imperial college press, (2004).

[2] A. K. Ali, "Preparation of Ag and Au Nanoparticles by Pulsed Laser Ablation in liquid," Sch. Appl. Sci. Univ. Technol. Iraq, Baghdad(2010).

[3] M. Abbasi and D. Dorranian, "Effect of laser fluence on the characteristics of Al nanoparticles produced by laser ablation in deionized water," Opt. Spectrosc., vol. 118, no. 3,(2015) pp. 472–481.

[4] P. K. Jain, K. S. Lee, I. H. El-Sayed, and M. A. El-Sayed, "Calculated absorption and scattering properties of gold nanoparticles of different size, shape, and composition: applications in biological imaging and biomedicine," J. Phys. Chem. B, vol. 110, no. 14,(2006) pp. 7238–7248.

[5] M. J Haider and M. S Mehdi, "Effect of Experimental Parameters on the Fabrication of Silver Nanoparticles by Laser Ablation," Eng. Technol. J., vol. 32, no. 4,(2014) pp. 704–709.

[6] A. K. Khan, R. Rashid, G. Murtaza, and A. Zahra, "Gold nanoparticles: synthesis and applications in drug delivery," Trop. J. Pharm. Res., vol. 13, no. 7,(2014) pp. 1169–1177.

[7] T. M. Al-Nori, "Antibacterial activity of Silver and Gold Nanoparticles against Streptococcus, Staphylococcus aureus and E. coli," Al-Mustansiriyah J. Sci., vol. 23, no. 3,(2012).

[8] A. K. Ali and D. N. Raouf, "Preparation of silver nanoparticles by pulsed laser ablation in liquid medium," J. Eng. Technol., vol. 29, no. 15,(2011) pp. 3058–3066.

[9] S. Al-Lami et al., "Micro fluidic Device for Cd Detection Using Gold Nano particles," Eng. Technol. J., vol. 32, no. 3 Part (B) Scientific,(2014).

[10] I. Alghoraibi and A. Alahmad, "Colloidal synthesis and structural characterizations of silver nanoparticles by using wet chemistry," Int. J. ChemTech Res., vol. 6, no. 1,(2014) pp. 871–880.

[11] G. Doria et al., "Noble metal nanoparticles for biosensing applications," Sensors, vol. 12, no. 2,(2012) pp. 1657–1687.

[12] E. Faoucher et al., "In situ preparation of network forming gold nanoparticles in agarose hydrogels," Chem. Commun., no. 43,(2009) pp. 6661–6663.

[13] A. L. Daniel-da-Silva, A. M. Salgueiro, and T. Trindade, "Effects of Au nanoparticles on thermoresponsive genipin-crosslinked gelatin hydrogels," Gold Bull., vol. 46, no. 1,(2013) pp. 25–33,.

[14] Y. Zhao and X. Jiang, "Multiple strategies to activate gold nanoparticles as antibiotics," Nanoscale, vol. 5, no. 18,(2013) pp. 8340–8350.

[15] A. N. Brown, K. Smith, T. A. Samuels, J. Lu, S. O. Obare, and M. E. Scott, "Nanoparticles functionalized with ampicillin destroy multiple-antibiotic-resistant isolates of Pseudomonas aeruginosa and Enterobacter aerogenes and methicillin-resistant Staphylococcus aureus," Appl. Environ. Microbiol., vol. 78, no. 8,(2012) pp. 2768–2774.

[16] R. A. Ismail, S. A. Zaidan, and R. M. Kadhim, "Preparation and characterization of aluminum oxide nanoparticles by laser ablation in liquid as passivating and anti-reflection coating for silicon photodiodes," Appl. Nanosci., vol. 7, no. 7,(2017) pp. 477–487.

[17] R. R. Letfullin, C. Joenathan, T. F. George, and V. P. Zharov, "Laser-induced explosion of gold nanoparticles: potential role for nanophotothermolysis of cancer,"(2006).

[18] P. Pandi and C. Gopinathan, "Structural transformation study of TiO2 nanoparticles annealing at different temperatures and the photodegradation process of eosin-Y," Phase Transitions, vol. 91, no. 4,(2018) pp. 406–425,.

[19] M. Murawska, A. Skrzypczak, and M. Kozak, "Structure and morphology of gold nanoparticles in solution studied by TEM, SAXS and UV-Vis," Acta Phys. Pol. A Gen. Phys., vol. 121, no. 4,(2012) p. 888.

[20] T. M. Rashid, U. M. Nayef, M. S. Jabir, and F. A. H. Mutlak, "Study of optical and morphological properties for Au-ZnO nanocomposite prepared by Laser ablation in liquid," in Journal of Physics: Conference Series, vol. 1795, no. 1, (2021) p. 12041.

[21] A. A. Al-Shamari, A. M. Abdelghany, H. Alnattar, and A. H. Oraby, "Structural and optical properties of PEO/CMC polymer blend modified with gold nanoparticles synthesized by laser ablation in water," J. Mater. Res. Technol., vol. 12,(2021) pp. 1597–1605,.

[22] R. K. Maeah, B. A. A.-H. Hasoon, A. I. Abdalwahab, K. F. F. Al-Azawi, and W. B. A. Hameedi, "Biosynthesis of silver nanoparticles using Hibiscus sabdariffa and their biological application," EurAsian J. Biosci., vol. 14, no. 2, (2020) pp. 3377–3383,.

[23] F. A. Fadhil, B. A. Hasoon, N. N. Hussein, and K. S. Khashan, "Preparation and characterization of CuO NPs via laser ablation under electric field and study their antibacterial activity," in AIP Conference Proceedings, vol. 2045, no. 1,(2018) p. 20002.

[24] Butheina A. Hasoon, Afnan I. Abdulwahab, Raghad Khwater Maeh, and Khalida F. Al-azawi, "Preparation and Characterization of Silver Nanoparticle by Cordia myxa Extract and their Study Anticancer, Antioxidant, Antibacterial Activity," Indian J. Forensic Med. Toxicol., vol. 15, no. 3 SE-Articles,(2021) pp. 5458–5465.

[25] Z. A. Sharba, B. A. Hasoon, R. K. Maeah, and N. N. Hussein, "Cytotoxicity, antioxidant, and antimicrobial activities of crude extract of quercus infectoria plant," Plant Arch, vol. 20,(2020) pp. 227–230.